

## Radiation-driven winds of hot luminous stars. Improvements of the theory and first results

A. Pauldrach, J. Puls, and R.P. Kudritzki

Universitäts-Sternwarte München, Scheinerstr. 1, D-8000 München 80, Federal Republic of Germany

Received October 18, 1985; accepted January 13, 1986

**Summary.** Selfconsistent model atmospheres of radiation-driven winds are constructed by means of two independent complementary codes. The first is based on the method of Castor et al. (1975, “CAK”), but uses the improved force multipliers calculated by Abbott (1982) and drops the crucial “radial streaming” approximation for the photons that drive the wind. The second involves a simultaneous solution of the hydrodynamics and the correct radiative transfer in the comoving frame (“CMF”) for a sample of weak, intermediate and strong lines at different wavelengths in the continuous spectrum. The latter code is used to test the validity of the CAK formalism, in particular the “Sobolev approximation”. The results are:

1. The “radial streaming” approximation is very poor and leads to completely unrealistic results. However, if this approximation is dropped, then the wind dynamics are changed significantly and much larger terminal velocities  $v_\infty$  are obtained. This effect removes the discrepancy between the observed and theoretical values of the ratio  $v_\infty/v_{\text{esc}}$  obtained with the old theory (see Abbott, 1982).

2. The CMF calculations yield results close to the improved CAK theory, thus allowing the tentative conclusion that for the wind dynamics the Sobolev approximation is not too bad. However this result will have to be refined by future calculations.

3. The effects of rotation are investigated and found to be small for main sequence O-stars, as long as  $v_{\text{rot}} < 200 \text{ km s}^{-1}$ .

4. For evolved O-stars with smaller gravities ( $\log g \leq 3.7$ ) the radiative line acceleration is still important in the photospheric layers and decreases the effective gravity. This can lead to systematic errors in the quantitative spectroscopy based on hydrostatic NLTE-models.

5. Detailed wind model calculations for individual stars show reasonable agreement with the observations for  $\dot{M}$  and  $v_\infty$ . This includes not only O-stars but also B-supergiants like the extreme object P-Cygni, where the high  $\dot{M}$  and low  $v_\infty$  are also reproduced by the calculations.

**Key words:** stars: atmospheres of, early-type, mass-loss

### 1. Introduction

Stellar winds are an ubiquitous feature of hot luminous stars. They dominate the ultraviolet spectra through the presence of

broad velocity-displaced absorption lines and they modify the photospheric energy distributions by additional free-free emission in the far IR- and radio-domain. The evolution of massive stars is strongly affected by the severe mass-loss connected with the stellar winds, which is reflected in the HR-diagrams of massive stars in the Milky Way as well as in the Magellanic Clouds and more distant galaxies. The stellar wind carries nuclear burned material back to the interstellar medium and provides an appreciable amount of energy, which influences the energy balance and causes additional star formation. Moreover, as recently pointed out by Abbott and Hummer (1985), the stellar winds also modify the structure of the underlying hydrostatic photospheres of the stars by scattering back a large part of the continuous photospheric radiation. The effect of this “wind-blanketing” is that the spectral types of massive stars do not depend only on effective temperature and gravity, but also on the density and extension of the surrounding stellar wind envelope. In practice, this means that effective temperature, gravity and mass-loss rate have to be determined simultaneously when hot stars are analyzed.

Consequently, the development of a quantitative theory for the winds of hot stars is of crucial astrophysical importance. Up to now, the most promising attempt is the theory of radiation driven winds. As demonstrated first by Lucy and Solomon (1970), the radiative momentum absorbed by UV spectral lines is able to initiate stellar winds, since the radiative line acceleration exceeds the gravity by a large factor. Abbott (1979) has shown that the domain in the HR-diagram where line-driven winds are self-initiating coincides with the domain where we observe mass-loss in hot stars. Castor, Abbott and Klein (1975, hereafter: CAK) in a pioneering outstanding paper developed the framework for a selfconsistent treatment of radiative driven wind model atmospheres. Although a number of drastic approximations entered into this work and only one model was calculated by CAK, these results have been used widely to prove or to disprove the radiation driven wind theory by comparison with observations. Usually in these comparisons no new calculations were made but only the scaling relations given by CAK for the mass-loss rate  $\dot{M}$  and the terminal velocity  $v_\infty$  were used. Thus much of the debate about the general reliability of radiation driven wind theory relies on the one model calculated by CAK and on the scaling relations.

One of the somewhat unrealistic approximations used by CAK was the representation of the line force by C III lines only. Here a major step forward was taken by Abbott (1982), who calculated line forces using a tabulation of lines which is complete for the elements H to Zn in the ionization stages I to VI.

Send offprint requests to: R.P. Kudritzki

Although the representation of the line force in this way was by far more realistic than that of CAK, significant discrepancies with the observations remained. In particular,  $\dot{M}$  was systematically too large for OB-stars by a factor of 2–3 and, more significantly,  $v_\infty$  was predicted to be only 1.1 to 1.3 times the escape velocity  $v_{\text{esc}}$  instead of the observed values of 2 to  $4v_{\text{esc}}$ . Since the measurement of  $v_\infty$  is relatively easy and normally not affected by large errors this latter discrepancy was very puzzling and cast doubt on the theory.

In addition, several other assumptions made in the CAK-theory were also subject to critical discussions. It was argued that the use of the Sobolev approximation throughout the atmosphere leads to inaccurate velocity fields and mass-loss rates (Weber, 1981, Leroy and Lafon, 1982). However, as the comparison between the CAK calculations and those by Weber and by Leroy and Lafon, who carried out exact radiative transfer calculations instead of the Sobolev approximations, were not done on a strictly differential basis this conclusion needs further critical investigation. In particular, Castor (private communication cited by Weber, 1981) pointed out that another approximation in the CAK-theory, namely the “radial streaming” of accelerating photons, might be more severe than the Sobolev approximation. (See also the recent review paper by Abbott, 1986).

The neglect of multiple scattering by CAK in calculating the line force was discussed by Panagia and Macchetto (1982) in a simple model, which predicted  $v_\infty \propto T_{\text{eff}}^2$ . However, in these calculations no consistent wind models were constructed and the back reaction of the multiple scattering on  $\dot{M}$  was not discussed. Friend and Castor (1983) recalculated one of the models by CAK taking into account multiple scattering in a statistical way. Much larger values for  $v_\infty$  were found (the individual values depending on the parametrisation of the line force), but again it is not clear whether these results reflect less the influence of multiple scattering than the dropping of the “radial streaming” approximation. In addition, no attempt has been made to compare the computed values of  $\dot{M}$  and  $v_\infty$  with observations. The importance of multiple scattering was also demonstrated in a recent paper by Abbott and Lucy (1985), who used Abbott’s (1982) line list, and adopted a fixed velocity field  $v(r)$  and a Monte Carlo technique for the multi line radiative transfer (see also Lucy, 1982a, 1983, 1984) to calculate the momentum transfer from the continuous photospheric radiation to the stellar wind plasma. By this method they were able to compute a mass loss rate for  $\zeta$  Puppis, which agrees well with the observed value. Moreover, the synthesized UV wind-spectrum of  $\zeta$  Puppis is in excellent agreement with the observations. However, the disadvantage of this method is – at least at the moment – that a velocity field has to be adopted in advance and, consequently, nothing is predicted for observable quantities like  $v_\infty$ .

This situation has motivated us to start a systematic study of radiation driven wind theory. For that purpose we have developed two independent complementary stellar wind codes, one of which uses the framework of the CAK theory allowing for certain improvements, and the other which calculates the radiative force and solves the hydrodynamic equations using a line-by-line solution of the exact radiative transfer equation in the comoving frame. The objective of the latter code for the future is to use explicitly Abbott’s full line list to calculate a realistic line force including multiple scattering. At the moment, a selected sample of weak, intermediate and strong lines longward and shortward of, and at the flux maximum, is used in the calculation. These

two codes at present allow a fairly systematic and comparative study of the importance of several approximations entering the radiation driven wind theory. This study is carried out in Sects. 2, 3 and 4. After a brief introduction of the basic equations (Sect. 2), in Sect 3 the CAK theory will be discussed. It will be shown that a rather simple modification of the theory by relaxing the “radial streaming” approximation already removes a large part of the conflict between the observed and calculated ratios of  $v_\infty/v_{\text{esc}}$ , as was encountered by Abbott (1982). Section 4 discusses the relative influence of exact radiative transfer calculations on the dynamics, if a sample of lines is chosen so that the total line force corresponds to Abbott’s force multiplier. In Sect. 5 it is demonstrated that the theory in the present stage is able to reproduce the observed values of  $\dot{M}$  and  $v_\infty$  for a representative sample of OB-stars, if the stellar parameters are adjusted within an “allowed range”. The conclusion (Sect. 6) is that the concept of radiation driven winds in a quantitative sense is very promising and that, consequently, it is worthwhile to improve the theory further by including in a consistent way multiple scattering, a realistic line list and more realistic ionisation calculations.

## 2. Basic equations and assumptions

As in the CAK theory we assume a radial symmetric stationary, one-component flow, ignoring viscosity and heat conduction. We will also neglect magnetic fields and rotation (except for the estimate given in Sect. 3). We are well aware that most of these simplifications (for a discussion see, for instance, Abbott, 1980) are normally subject to some qualitative criticism which, however, is rarely specified in a quantitative sense. We feel that the basic principles of the simple theory have to be worked out properly before we can start to improve it by including additional effects. In hot luminous stars the overwhelming presence of the radiative force is observationally manifested (see for instance, Lamers and Morton, 1976). Magnetic fields of considerable strength, which could modify the dynamics, are however not observed. (We will discuss the paper by Friend and MacGregor (1984) in Sect. 3). Rotation can modify the wind but is of minor importance for main sequence O-stars as long as the rotation velocities are below  $200 \text{ km s}^{-1}$  (see Sect. 3).

From the observation of drifting narrow line components in the P-Cygni profiles (Henrichs, 1984; Howarth and Prinja, 1985) it is evident that winds of hot luminous stars are in principle not stationary. It is clear that our stationary wind theory is not able to explain these features, but can describe only the time averaged wind properties which account for the general overall more or less stable shape of the P-Cygni profiles of hot luminous stars. On the other hand a good stationary theory might be useful for a refined stability analysis of stellar winds, which then could lead to an improved understanding of the variability.

Lucy and White (1980) and Lucy (1982b) were able to show that in a two-component treatment of the wind, shocks can be formed which travel through the wind and cause non-monotonic flows. These shocks most probably are responsible for the observed O-stars X-rays, the super-ionization in the wind and the wide black absorption trough in the observed P-Cygni profiles (Lucy, 1983, 1984). At the moment, we are not able to treat these shocks in self-consistent wind-model calculations. Fortunately, the numerical experiments by Abbott and Lucy (1985) show that the general dynamics of the wind are not strongly affected by

the presence of these shocks. We therefore conclude that, at least at present, the neglect of shocks is not important, and consequently will assume a one-component flow in radiative equilibrium. The observational evidence for such cool wind flows (outside the shocks!) comes from recent IR-data (Abbott et al., 1984a; Lamers and Waters, 1984). According to our test calculations (see also Abbott, 1986, who obtained similar results) the temperature structure is not crucial for the wind dynamics (see Sects. 3 and 4). We therefore use the spherical grey temperature distribution in the approximation given by Lucy (1971):

$$T^4(R_*/r) = T_{\text{eff}}^4(r = R_*)(W + (3/4)R_* \int_0^{R_*/r} \bar{\chi}_H d(R_*/r)). \quad (1)$$

$r$  is the radial coordinate,  $R_*$  the photospheric radius (defined by a certain optical depth, for instance  $\tau(R_*) = \int_1^\infty \bar{\chi}_H d(r/R_*) = 1$ ,  $W = 0.5(1 - (1 - (R^*/r)^2)^{1/2})$  the dilution factor and  $T_{\text{eff}}$  the effective temperature at the photospheric radius.  $\bar{\chi}_H$  is the flux weighted mean of the opacity.

The stellar wind is then described by the conservation of mass and the momentum equation:

$$\dot{M} = 4\pi r^2 \rho(r) v(r), \quad (2)$$

$$v \frac{dv}{dr} = -\frac{1}{\rho(r)} \frac{dp}{dr} - \frac{GM_*}{r^2} + g_{\text{rad}}. \quad (3)$$

$v(r)$ ,  $\rho(r)$ ,  $p(r)$  are the velocity, density and pressure, respectively,  $M_*$  is the stellar mass and  $G$  the gravitational constant. The radiative acceleration  $g_{\text{rad}}$  is given by

$$g_{\text{rad}} = \frac{1}{c\rho(r)} \left( \sigma_{\text{Th}}(r) \sigma_B T_{\text{eff}}^4(r) + 4\pi \int_0^\infty \chi_v^C(r) H_\nu(r) d\nu + 4\pi \sum_{\text{all lines}} \int_0^\infty H_\nu(r) \chi_\nu^L(r) d\nu \right). \quad (4)$$

The first term takes into account Thomson scattering ( $\sigma_{\text{Th}}$  is the electron scattering absorption coefficient,  $\sigma_B$  the Stefan-Boltzmann constant), the second represents bound-free and free-free absorption ( $\chi_v^C$  is the absorption coefficient,  $H_\nu$  the monochromatic Eddington flux) and the third term describes the line force. ( $\chi_\nu^L$  is the absorption coefficient for one individual line). In the following sections we describe the alternative treatments of this third term.

### 3. The modified CAK-theory (MCAK)

#### 3.1. The approximations of the CAK-theory

In describing the radiative acceleration provided by a single line, the theory of CAK makes use of four approximations:

##### 3.1.1. The Sobolev approximation (SA)

This approximation, which is valid only for supersonic velocities and large velocity gradients, leads to the following expression for  $g_{\text{rad}}$  of a single line

$$g_{\text{rad}}^L = \frac{2\pi}{c\rho(r)} \Delta v_D \bar{\chi}_L(r) \int_{-1}^1 I_c(r, \mu) \frac{1 - e^{-\tau_S(r, \mu)}}{\tau_S(r, \mu)} \mu d\mu. \quad (5)$$

Here,  $\chi_L(r)$  is defined by

$$\chi_L^L(r) = \bar{\chi}_L(r) \varphi \left( \frac{v - v_0}{\Delta v_D} \right), \quad (6)$$

where  $\varphi$  is the Doppler-broadening function and  $\Delta v_D$  the Doppler width. The ‘‘Sobolev optical depth’’  $\tau_S(r, \mu)$  is then given by

$$\tau_S(r, \mu) = \frac{\bar{\chi}_L(r) v_{\text{th}}}{(1 - \mu^2)v/r + \mu^2 dv/dr}. \quad (7)$$

Here  $I_c(r, \mu)$  is the specific continuous intensity at the line frequency at the radial coordinate  $r$ , and  $\mu$  is the usual cosine of the angle between the ray direction and the outward normal on the spherical surface element.

##### 3.1.2. Core-halo structure of photosphere and wind

If the hydrostatic photosphere, where the continuum is formed, is well separated from the line forming region, we can assume

$$\frac{\delta I_c}{\delta r} = 0 \quad (8)$$

in this region.

##### 3.1.3. No limb-darkening

If we neglect photospheric limb darkening (see also Castor and Lamers, 1979), we obtain

$$\frac{\delta I_c}{\delta \mu} = 0. \quad (9)$$

With Eqs. (8) and (9) equation (5) reduces to

$$g_{\text{rad}}^L = \frac{2\pi}{c\rho(r)} \bar{\chi}_L(r) \Delta v_D I_c(R_*) \int_{\mu_*}^1 \frac{1 - e^{-\tau_S(r, \mu)}}{\tau_S(r, \mu)} \mu d\mu. \quad (10)$$

$\mu_*$  is then defined by

$$\mu_* = (1 - (R_*/r)^2)^{1/2}. \quad (11)$$

##### 3.1.4. The ‘‘radial streaming’’ of photons

CAK assumed that most of the momentum would be provided by ‘‘radial streaming’’ of photons. By this approximation, which neglects the finite cone angle of the radiating photospheric surface, the Sobolev optical depth becomes independent of  $\mu$  and reads

$$\tau_S(r) := \tau_S(r, \mu = 1) = \frac{\bar{\chi}_L(r) v_{\text{th}}}{dv/dr}. \quad (12)$$

Accordingly, Eq. (10) reduces to

$$g_{\text{rad}}^L(\tau_S(r)) = \frac{\pi}{c\rho(r)} \bar{\chi}_L(r) \Delta v_D I_c(R_*) \frac{1 - e^{-\tau_S(r)}}{\tau_S(r)} (R_*/r)^2. \quad (13)$$

It is clear that Eq. (13) will hold at very large radii, where the star appears as a point source. However, in the crucial region close to the photospheric surface and out to a few stellar radii this approximation is very crude. This is demonstrated best by introducing the correction factor

$$\text{CF} = g_{\text{rad}}^L(\tau_S(r, \mu)) / g_{\text{rad}}^L(\tau_S(r)). \quad (14)$$

It is obvious that

$$\begin{aligned} \text{CF} < 1, & \quad \text{if } \frac{dv}{dr} > \frac{v}{r} \\ \text{CF} > 1, & \quad \text{if } \frac{dv}{dr} < \frac{v}{r} \end{aligned} \quad (15)$$

$$\text{CF} = 1, \quad \text{if } \frac{dv}{dr} = \frac{v}{r} \rightarrow 0.$$

Assuming a strong line ( $\tau_s \gg 1$ ) and a velocity field of the form  $v(r) = v_\infty(1 - R_*/r)^{1/2}$  (as obtained approximately by CAK) the correction factor can be easily calculated. It is displayed in Fig. 1, which shows that close to the photospheric surface the correct force is much smaller than in the radial streaming approximation, whereas at some stellar radii CF becomes larger than unity. This behaviour of the radiative acceleration significantly modifies the stellar wind dynamics relative to the radial streaming approximation of CAK.

### 3.2. CAK-theory with finite cone angle correction factor

Using Eqs. (12) and (13) and an elaborate line list of the C III ion whose abundance was chosen so to be representative of the total amount of C, N and O, CAK calculated a total line force by summing over all strong and weak lines. They showed that this sum can be parametrized by

$$g_{\text{rad}}^L = \frac{1}{c\rho(r)} \sigma_{\text{Th}}(r) \sigma_B T_{\text{eff}}^4(r) M_{\text{CAK}}(t). \quad (16)$$

where the “force-multiplier”  $M(t)$  – the line force in units of Thomson-scattering force – is given by

$$M_{\text{CAK}}(t) = kt^{-\alpha}. \quad (17)$$

Here the constants  $k$  and  $\alpha$  represent the number of lines present and the ratio of weak to strong lines, respectively (see also Abbott, 1980). CAK used mean values  $\bar{k} = 1/30$  and  $\bar{\alpha} = 0.7$ . The depth parameter  $t$  is defined by

$$t = \sigma_e \rho v_{\text{th}} (dv/dr)^{-1} \quad (18)$$

where

$$\sigma_e = \frac{\sigma_{\text{Th}}}{\rho}.$$

( $v_{\text{th}}$  is the thermal velocity of the carbon ion). Setting  $t$  proportional only to  $(dv/dr)^{-1}$  gives the radial streaming approximation (Eqs. (12), (13)). As indicated by CAK (see their Eq. 49) one can avoid this by using the “exact” depth parameter

$$t_{\text{ex}} = t \frac{dv}{dr} \left/ \left( (1 - \mu^2) \frac{v}{r} + \mu^2 \frac{dv}{dr} \right) \right., \quad (19)$$

which then leads to the improved force multiplier

$$\bar{M} = (2/(1 - \mu_*^2)) \int_{\mu_*}^1 M_{\text{CAK}}(t_{\text{ex}}) \mu d\mu \quad (20)$$

or explicitly gives

$$\bar{M}(t, v, dv/dr, r) = M(t) (2/(1 - \mu_*^2)) \times \int_{\mu_*}^1 \left( \left( (1 - \mu^2) \frac{v}{r} + \mu^2 \frac{dv}{dr} \right) \frac{dv}{dr} \right)^\alpha \mu d\mu. \quad (21)$$

CAK did not, however, use this improved force multiplier  $\bar{M}$  because it complicates the equation of motion significantly. If we follow the notation of CAK and define

$$\begin{aligned} w &= \frac{1}{2}v^2 \\ w' &= dw/du \\ u &= -1/r \end{aligned} \quad (22)$$

$$h(u) = -GM(1 - \Gamma) - 2a^2/u - da^2/du$$

( $a$  is the isothermal sound speed, i.e.  $p = a^2\rho$  and  $\Gamma = \sigma_e \sigma_B T_{\text{eff}}^4(r)r^2/(GMc)$ , Eqs. (2), (3), (16), (17) or (21) yield (neglecting the bound-free and free-free force)

$$F(u, w, w') \equiv (1 - a^2/2w)w' - h(u) - CK(u, w, w')(w')^\alpha = 0, \quad (23)$$

where the constant  $C$  (the eigenvalue of the problem) is given by

$$C = \Gamma GMk(4\pi/(\sigma_e v_{\text{th}} \dot{M}))^\alpha. \quad (24)$$

In the radial streaming approximation of CAK (eq. 17) we have  $K(u, w, w') = 1$ . However, taking into account the finite cone angle of the photospheric disk (eq. 21) we obtain

$$K(u, w, w') = \begin{cases} (1 - (1 - R_*^2 u^2 - 2R_*^2 w u/w')^{\alpha+1}) / ((\alpha + 1) R_*^2 u^2 (1 + 2w/w' u)) & \text{for } r > R_* \\ (1 - (2R_* w/w')^{\alpha+1}) / ((\alpha + 1)(1 - 2wR_*/w')) & \text{for } r \leq R_*. \end{cases} \quad (25)$$

We have solved the wind Eqs. (23) and (25) in a way analogous to CAK starting from the “critical point” of Eq. (23) (for details of the computations, see Appendix). We first recalculated the wind model for a typical O5V-star using the same parameters as CAK:  $\log g = 3.94$ ,  $R_* = 13.8 R_\odot$ ,  $T_{\text{eff}}(R_*) = 49290 \text{ K}$ . The results are summarized in Table 1, where the mass loss rate  $\dot{M}$ , the

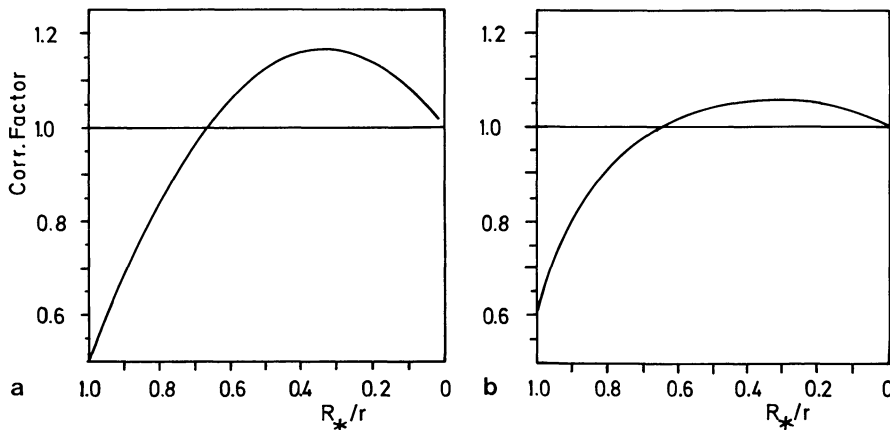


**Fig. 1a and b.** The correction factor (see eq. 14) for a velocity field  $v(r) = v_\infty(1 - R_*/r)^{1/2}$  and a strong (a) and weak (b) line

**Table 1.** Stellar wind properties for a typical 05V-star using the CAK force-multiplier

Model	$\dot{M}$ ( $10^{-6} M_{\odot}/\text{yr}$ )	$v_{\infty}$ $\text{km s}^{-1}$	$r_c/R_*$	$v_c$ $\text{km s}^{-1}$	$v(R_*)$ $\text{km s}^{-1}$	$\dot{M}v_{\infty}c/L$
Radial streaming $K \equiv 1$ $T(r) = T_{\text{eff}}(R_*)$	6.7	1559	1.568	844	0.2	0.53
Radial streaming $K \equiv 1$ $T(r)$ with Eq. (1)	6.7	1468	1.945	991	0.21	0.50
Finite cone angle $K(u, w, w')$ with Eq. (25) $T(r) = T_{\text{eff}}(R_*)$	3.52	5123	1.023	144	0.094	0.92
Finite cone angle $K(u, w, w')$ with Eq. (25) $T(r)$ with Eq. (1)	3.48	5271	1.020	135	0.094	0.93

terminal velocity  $v_{\infty}$ , the radius of the critical point  $r_c$ , the velocity at the critical point  $v_c$ , the photospheric velocity  $v(R_*)$  and the “wind efficiency”  $\dot{M}v_{\infty}c/L$  are given. For the radial streaming approximation ( $K \equiv 1$ ) we obtain results which are nearly identical with CAK, who found  $\dot{M} = 6.6 \cdot 10^{-6} M_{\odot}/\text{yr}$  and  $v_{\infty} = 1515 \text{ km s}^{-1}$ . The detailed choice of the temperature structure is of minor importance since the model with  $T(r) = T_{\text{eff}}(R_*) = \text{const.}$  leads to results very similar to those with  $T(r)$  specified by eq. (1). (The position of  $r_c$  depends of course on  $T(r)$ , but this has no influence on the final solution).

With the correct angle integration in the radiative force (eq. (25)), however, the situation changes completely (see also Abbott, 1986). We obtain a smaller  $\dot{M}$  and a significantly larger  $v_{\infty}$ . (Fig. 2 shows the density-, velocity- and temperature structure for the two cases). This is explained by the run of the correction factor  $K(u, w, w')$ , which is plotted in Fig. 3. In deeper layers, where the mass loss rate is fixed,  $K$  is smaller than unity (see also the preceding section). This results in a smaller  $\dot{M}$ , since the driving force is smaller. In the outer layers we have  $K > 1$ , which means that the gas flow (which also has lower density than in the  $K \equiv 1$  case, since  $\dot{M}$  is smaller) experiences a stronger acceleration. This yields a larger  $v_{\infty}$ .

However, compared with typical observed values of  $v_{\infty}$  for 05V-stars, which are between 2000 and 3000  $\text{km s}^{-1}$ , the terminal velocity of 5000  $\text{km s}^{-1}$  obtained with the correct, angle-integrated line force is completely unrealistic. This is caused by the values of  $\bar{k}$  and  $\bar{\alpha}$ , which were obtained by representing the line force through C III lines only. As we shall show below, the situation is much improved if Abbott’s (1982) force multipliers are used. Ironically, the original pioneering CAK theory – although being the qualitative break-through in the consistent theoretical treatment of the problem – led quantitatively to results not too far from observations only because two not-too-good approximations compensated each other: the “radial streaming” of photons and the line force given by C III lines only.

### 3.3. Stellar wind models, with the Abbott-force-multiplier and finite cone angle correction factor

Abbott (1982) calculated new force multipliers based on a line list which is essentially complete for the first to sixth stages of ionization of the elements from H to Zn. Moreover, he included a more realistic treatment of the radiative ionization of elements in the stellar winds, which leads to an additional dependence of the

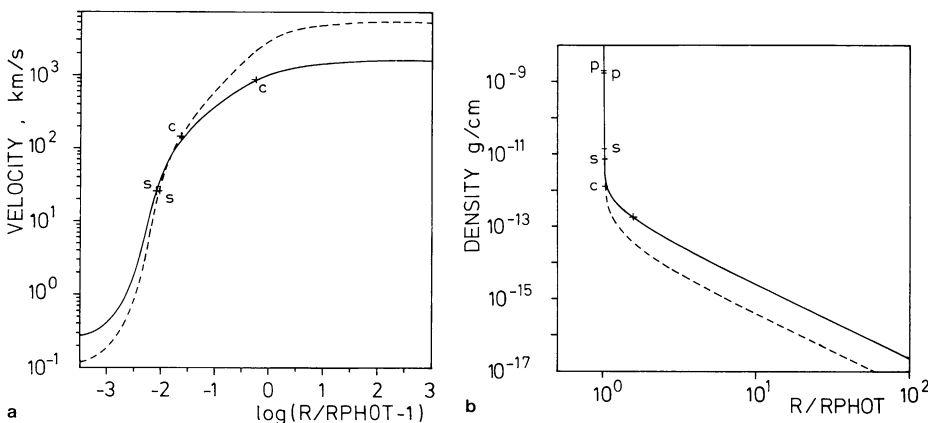


**Fig. 2a and b.** Velocity (a) and density (b) structure of a typical 05f star derived from the CAK-theory. Calculations with the radial streaming approximation are fully drawn, whereas the results obtained with the correction factor are represented by the dashed curve. The dots labelled C, S and P are the critical, sonic and photospheric points, respectively

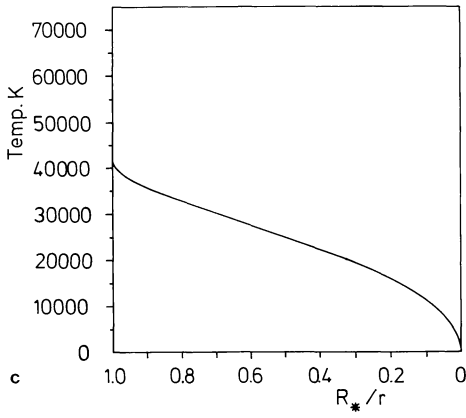


Fig. 2c. Temperature structure for the 05f-star

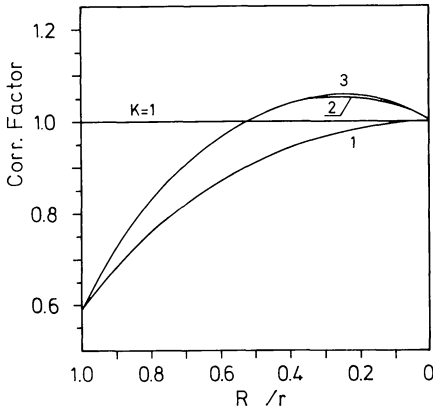


Fig. 3. The correction factor  $K(u, w, w')$  (curve 3) for the 05f-star.  $K(u, w, w')$  is calculated iteratively (see Appendix). The starting approximation (curve 1) and the next step (curve 2) are also shown

force multiplier on electron density  $n_E$  (in  $10^{11} \text{ cm}^{-3}$ ) and dilution factor  $W$ :

$$M_A(t) = kt^{-\alpha}(n_E/W)^\delta. \quad (26)$$

Taking the individual values of  $M_A(t)$  for  $T_{\text{eff}} = 50000 \text{ K}$  and  $40000 \text{ K}$  in Abbott's Table 2 for the relevant values of  $t$ , we obtain  $k = 0.124$ ,  $\alpha = 0.64$ ,  $\delta = 0.07$  for the typical 05V-star of the above section (see also Section 5). (Following the redefinition by Abbott the thermal velocity of hydrogen has to be used in the calculation of the depth parameter  $t$  according to Eq. (18)). In the radial streaming approximation this would lead to  $v_\infty =$

$(\alpha/(1-\alpha))^{1/2}v_{\text{esc}} = 1.3v_{\text{esc}}$  (CAK, Abbott, 1978; Abbott, 1982), where  $v_{\text{esc}} = (2GM/R_*(1-\Gamma))^{1/2}$  is the photospheric escape velocity and has the value of  $975 \text{ km s}^{-1}$  for our 05V-star. Consequently, for this example, the radial streaming approximation yields  $v_\infty = 1270 \text{ km s}^{-1}$  with Abbott's improved force multiplier, a value much too small when compared with observations (see also Abbott's Fig. 9).

However, with the correct finite-cone angle integration we obtain a much better result. When we integrate the modified CAK equation of motion, which now using Eqs. (26) in (21) reads

$$F(u, w, w') \equiv (1 - a^2/2w)w' - h(u) - CG(u, w, w')w^{-\delta/2}(w')^\alpha = 0$$

$$G(u, w, w') = K(u, w, w') \begin{cases} ((1 - (1 - R_*^2 u^2)^{1/2})/u^2)^\delta & \text{for } r > R \\ (1/u^2)^\delta & \text{for } r \leq R_* \end{cases} \quad (27)$$

$$C = \Gamma GMk2^{-\delta/2}(D\dot{M}/2\pi)^\delta(4\pi/(\sigma_e v_{\text{th}} \dot{M}))^\alpha$$

$$D = (1 + I_{\text{He}} Y_{\text{He}})/((1 + 4Y_{\text{He}})m_{\text{H}}(10^{11} \text{ cm}^{-3}))$$

$$Y_{\text{He}} = 0.1 = \text{number ratio of He to H}$$

$$I_{\text{He}} = 2 = \text{number of free electrons provided by a helium atom}$$

$$m_{\text{H}} = \text{mass of hydrogen atom,}$$

we find the values given in Table 2 (for details of the computations see Appendix). The value of  $v_\infty = 2900 \text{ km s}^{-1}$ , which is now obtained, is much closer to the observations and the mass-loss rate is also reasonable.

This result is very satisfying, because it shows that the enormous effort by Abbott (1982) in calculating a line force from a realistic line list yields a significant improvement in the reliability of the results, if the theory is applied correctly and the radial streaming approximation is relaxed. Although further improvements such as the correct inclusion of multiple scattering and a more realistic treatment of the occupation numbers will be necessary, we find it worthwhile at the present stage of development to compare for individual stars the predictions of the theory concerning  $\dot{M}$  and  $v_\infty$  with the observations. This will be discussed in detail in Sect. 5.

### 3.4. Influence of stellar rotation and magnetic fields on the dynamics

As the effect of stellar rotation on radiatively-driven stellar winds is an unpleasant problem in the exact three-dimensional case, we have considered some approximations.

First we assumed the flow to have a zero component of velocity in latitude. This gives

$$v = v_r(r)r + v_\phi(r)\Phi. \quad (28)$$

Table 2. Stellar wind properties for a typical 05V-star using the Abbott force-multiplier

Model	$\dot{M}$ ( $10^{-6} M_\odot/\text{yr}$ )	$v_\infty$ $\text{km s}^{-1}$	$r_c/R_*$	$v_c$ $\text{km s}^{-1}$	$v(R_*)$ $\text{km s}^{-1}$	$\dot{M}v_\infty c/L$
Finite cone angle $G(u, w, w')$ with Eq. (26) $T(r) = T_{\text{eff}}(R_*)$	6.76	2915	1.04	184	0.2	1.00
Finite cone angle $G(u, w, w')$ with Eq. (26) $T(r)$ with Eq. (1)	6.70	2900	1.037	178	0.22	0.99

Second we took the angular momentum per unit mass  $P$  to be conserved. That means

$$rv_\phi = P = R_* v_{\text{rot}}. \quad (29)$$

As a result of the first approximation, we expect the three-dimensional treatment of stellar rotation to lie between our results for the cases with and without rotation. As for Eq. (29), we are well aware that turbulent viscosity will violate the conservation of angular momentum in the region where  $v_r < a$ . But as this region is very near to the photosphere,  $P$  would be modified only in a negligible way.

With these assumptions the effect of rotation can be described by inserting a known centrifugal term into the equation of motion. So Eq. (22) is now given by

$$h_{\text{rot}}(u) = h(u) - R_*^2 v_{\text{rot}}^2 u. \quad (30)$$

Figure 4 shows the dependence of  $v_\infty$  and  $\dot{M}$  versus  $v_{\text{rot}}$  for the assumed typical O5V-star.

As can be seen, the wind parameters vary by only a few percent as long as  $v_{\text{rot}}$  is less than  $200 \text{ km s}^{-1}$ , which is a realistic value for O-stars. Our results give a weaker dependence of  $v_\infty$  on  $v_{\text{rot}}$  than those of Castor (1978). This can be explained as the consequence of our angular correction factor, which puts the critical point closer to the sonic point. Our results imply that at least for normal O-stars it is not necessary to investigate the influence of rotation on stellar wind dynamics in a more elaborate way.

One of our basic assumptions in Sect. 2 was to neglect magnetic fields. As has been recently shown by Friend and MacGregor (1984) (hereafter FG), this can be *a priori* dangerous. Therefore we think it necessary to comment on the investigation of FG in view of our results:

The motivation for the work of FG was the discrepancy between the observed values of  $v_\infty$  and the predictions by the CAK theory,

as pointed out by Abbott (1982) and discussed in the foregoing sections. In their interesting treatment of radiation driven winds in the presence of magnetic fields and rotation FG were able to show that in fact this discrepancy disappears, if magnetic fields of considerable strengths (Kilogauss) are adopted. On the other hand, the wind dynamics remain nearly unchanged, as long as the magnetic fields are of the order of some hundred Gauss. Their conclusion was that the contribution of (yet unobserved) strong magnetic fields and rotation might be responsible for the observed O-star wind velocities. However, in those calculations the old CAK-representation for the line force was used, which is based on the radial streaming approximation. Since we were able to show that avoiding this approximation by the use of the finite cone angle correction factor changes the wind dynamics drastically and leads to values close to the observations (see also Sect. 5), we conclude that it is not necessary to consider such strong magnetic fields as long as they are not observed.

### 3.5. Scaling relations for $\dot{M}$ and $v_\infty$

In their 1975 paper CAK derived simple scaling relations for  $v_\infty$  and  $\dot{M}$  (their Eqs. 47, 42)

$$v_\infty = (\alpha/(1-\alpha))^{1/2} v_{\text{esc}}$$

$$\dot{M} = (4\pi GM/\sigma_e v_{\text{th}}) \alpha (1-\alpha)^{(1-\alpha)/\alpha} (k\Gamma)^{1/\alpha} (1-\Gamma)^{-(1-\alpha)/\alpha}$$

As pointed out in Sects. 3.2, and 3.3, these relations fail when compared with observations. In particular, the values for  $\alpha$  obtained by CAK and Abbott ( $\alpha = 0.7$ ;  $0.56$  respectively) imply

$$v_\infty = 1.53(1.02)v_{\text{esc}}$$

which is much too small to account for the observed terminal velocities of order two to four times  $v_{\text{esc}}$  (Abbott, 1982).

For an easy comparison with observations, we developed new scaling relations for our MCAK-theory with Abbott's force multiplier (for details see Appendix):

$$\dot{M} = (c_1(2\pi/D)^\delta (\sigma_e v_{\text{th}}/4\pi)^\alpha / (k\Gamma GM 2^{-\delta/2}))^{1/(\delta-\alpha)}$$

$$c_1 = (GM(1-\Gamma))^{1-\alpha} (1.36 \cdot 10^7 R_*^2)^\delta (1-\alpha)^{\alpha-1} \alpha^{-\alpha} \times (\alpha+1) 0.9(1-0.1^{\alpha+1}) \quad (31)$$

(see also Eq. 27). For  $v_\infty$ , we could not find a simple result analogous to that derived by CAK, because the radius-dependence of the correction factor prohibits a quasi-analytical solution.

Instead, we obtained a semi-empirical formula by calculating  $v_\infty$  in three steps.

1. A few simplifications of the MCAK equations (see also Appendix) yield in an approximate expression for the critical velocity:

$$v_{\text{crit}} = (\alpha/(1-\alpha))^{1/2} (\delta/(4fc(u_c)))^{1/2} v_{\text{esc}} \quad \text{for } v_{\text{crit}} \gg v_{\text{sound}} \quad (32)$$

$$fc(u_c) = 1 - (1 - u_c^2 R_*^2)^\alpha (1 + \alpha)$$

2. Assuming a power law for the velocity field which is justified only afterwards by the results

$$v(r) = v_\infty (1 - R_*/r)^\beta, \quad (33)$$

and approximating the location of the critical point as  $r_c \approx 1.04R_*$ , one gets  $v_\infty = v_{\text{crit}}(1 - 1/1.04)^{-\beta}$  with  $\beta$  as an up-to-now unknown parameter (CAK found  $\beta = 1/2$ ).

3. Using a grid of 150 models in the range of  $T_{\text{eff}} = 20000 - 50000 \text{ K}$ , we found that  $\beta$  (in the layers above the critical point)

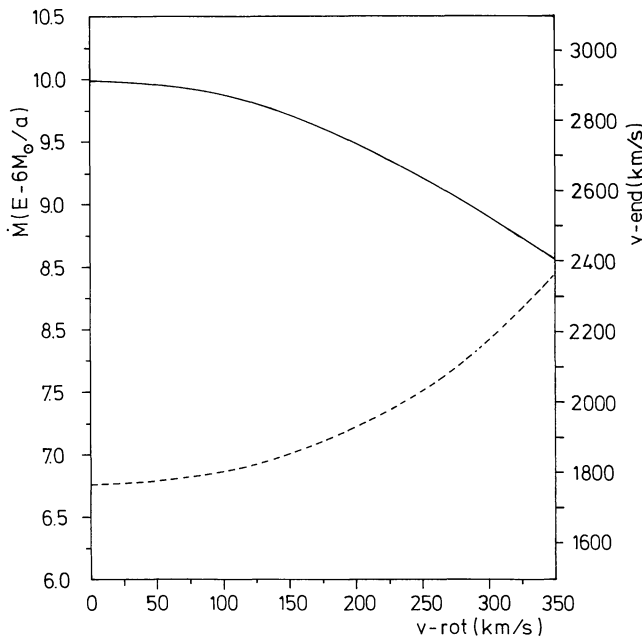


Fig. 4. The dependence of  $\dot{M}$  (dashed) and  $v_\infty$  (fully drawn) on  $v_{\text{rot}}$  for the O5F-star

depended mainly on  $\alpha$ ,  $\delta$ ,  $v_{\text{esc}}$  and could be represented by the fit-formula

$$\beta = 0.97\alpha + 0.032v_{\text{esc}}/500 \text{ km s}^{-1} + 0.008/\delta \quad (34)$$

where  $\alpha$  and  $\delta$  are functions of  $T_{\text{eff}}$  and  $g$ , discussed in Sect. 5.

Therefore, our final expression for  $v_{\infty}$  is

$$v_{\infty} = v_{\text{crit}}(1 - 1/1.04)^{-(0.96\alpha + 0.032v_{\text{esc}}/500 \text{ km s}^{-1} + 0.008/\delta)} \quad (35)$$

with  $v_{\text{crit}}$  from Eq. 32.

As an interesting by-product, we found that the velocity parameter  $\beta$  for stars with  $T_{\text{eff}} = 40000 - 50000 \text{ K}$  is nearly equal 0.80, so that the power law

$$v(r) = v_{\infty}(1 - R_{\star}/r)^{0.80}$$

for some approximate calculations may be justified. In Table 5 we compare results from our new scaling relations to those determined numerically for MCAK for selected stars, the parameters of which are also discussed in Sect. 5. One finds a maximum deviation at the 5% level.

Two points must be stressed:

Contrary to CAK's results, we find a slightly non-linear dependence of  $v_{\infty}$  on  $v_{\text{esc}}$ , which indicates that no simple expression for the case with correction factor is possible.

Secondly, we have not yet investigated the dependence of the CAK-parameters on metallicity, which will obviously greatly influence  $k$  and  $\alpha$ . Therefore, the above relation for  $v_{\infty}$  should be applied to objects with solar abundance only. In a forthcoming paper we will return to the problem of the metallicity dependence.

#### 4. Radiation-driven wind dynamics using comoving frame calculations for the radiative force (CMF)

In this section we will present our second method of calculating stellar wind models, using the comoving frame (CMF) method to evaluate the line acceleration, and compare the results to those obtained by the MCAK theory based on the SA radiative transfer. As we are mainly interested in the radiation force, our choice of the CMF method is a natural one, because in this way we get a simple expression for that quantity, as the opacities and emissivities become functions of radius and frequency alone.

##### 4.1. The radiative force of a single line

Following the development of Mihalas et al. (1975, 1976), in spherically symmetric atmospheres with stationary flows the equation of transfer for radiation as seen by an observer comoving with the gas is given (in order  $v/c$ ) by

$$\begin{aligned} \mu \frac{\partial}{\partial r} I(v, \mu, r) + \frac{1 - \mu^2}{r} \frac{\partial}{\partial \mu} I(v, \mu, r) - \frac{v_0}{c} \left( (1 - \mu^2) \frac{v}{r} + \mu^2 \frac{dv}{dr} \right) \frac{\partial I}{\partial v} \\ = \eta(v, r) - \chi(v, r)I(v, \mu, r) \end{aligned} \quad (36)$$

with

$I(v, \mu, r)$	specific intensity
$\mu$	direction cosine between radiation and flow
$v(r)$	radial flow speed
$v_0$	observer's line frequency
$\eta$	total emissivity
$\chi$	total opacity

per unit volume.

The line emission is described by a source function (complete redistribution is assumed) of the form

$$S_L(v, r) = \zeta(v, r) \int J(v, r) \Phi(v, r) dv + \psi(v, r). \quad (37)$$

Here  $\zeta$  and  $\psi$  are specified functions dependent on the atomic transition and  $\Phi$  is the appropriate line profile.

The principle of calculating the line force is as follows. After evaluating the specific intensity arising from continuum processes at the blue wing frequency of the line, we calculate as an initial value the line source function using the Sobolev theory with continuum (Hummer and Rybicki, 1985; Hummer and Puls, in prep.).

With this we solve the CMF transfer equation and get Eddington factors  $f_v$  and  $g_v$ , defined by

$$f_v = K_v/J_v, \quad g_v = N_v/H_v$$

where

$$(J_v, H_v, K_v, N_v) = \frac{1}{2} \int_{-1}^{+1} d\mu I_v(\mu)(1, \mu, \mu^2, \mu^3). \quad (38)$$

As a lower boundary we use the diffusion approximation at an optical depth in Thomson scattering  $\tau_{\text{TH}} = 10$ , and as an outer boundary we specify no incident radiation from above. The next step is to solve the angular moment equations of (36)

$$\frac{1}{r^2} \frac{\partial(r^2 H_v)}{\partial r} - \frac{v_0}{c} \left( \frac{v}{r} \frac{\partial(1 - f_v)J_v}{\partial v} + \frac{dv}{dr} \frac{\partial(f_v J_v)}{\partial v} \right) = \eta_v - \chi_v J_v, \quad (39)$$

$$\begin{aligned} \frac{\partial(f_v J_v)}{\partial r} + \frac{(3f_v - 1)}{r} J_v - \frac{v_0}{c} \left( \frac{v}{r} \frac{\partial(1 - g_v)H_v}{\partial v} + \frac{dv}{dr} \frac{\partial(g_v H_v)}{\partial v} \right) \\ = -\chi_v H_v \end{aligned} \quad (40)$$

in order to obtain a new value for  $J_v$  and therefore also for  $S_L$ . This process is iterated until convergence (normally 3–4 iterations needed for a precision better than 3%). Calculating the transfer equation with the correct line-source function a last time, we obtain the first moment of the specific intensity  $H_v$  and with this the radiative acceleration in the observers frame

$$g_{\text{rad}}^L(r) = \frac{4\pi}{c\rho(r)} \int \bar{\chi}_v^L(r) \Delta v_D H_v(r) \Phi(v, r) dv. \quad (41)$$

In Fig. 5 we compare the “exact” line acceleration derived in this way with that resulting from the Sobolev approximations in order to examine how far we can trust the results of the MCAK theory. (The model star we used is described in Sect. 3.2). Radiative accelerations are shown for a strong and a weak line ( $\eta_L = 10^5, 10^2$ , see Sect. 4.2) arising from the CMF method (—), from the SA with correct continuum intensity (see Eq. 5, ...) and the SA without continuum neglecting limb darkening (see Eq. 10, ---), where  $I_c$  is given by

$$I_c = 4H_v^{\text{em}} R_{\text{max}}^2 \quad (42)$$

with  $H_v^{\text{em}}$  the emergent flux of the continuum radiation field at the blue wing frequency at  $r = R_{\text{max}}$  (usually  $100R_{\star}$ ). (The latter treatment of the radiative transfer was used in the calculation of the force multipliers discussed in the foregoing sections). It can be seen that for the outer regions ( $r > 1.3R_{\star}$ ) all three calculations are in perfect agreement due to the fact that the SA in regions where  $v \gg v_{\text{sound}}$  is very accurate. On the other hand, in the deepest layers we have the largest deviations, as the CMF-force is bounded by the diffusion approximation whereas the



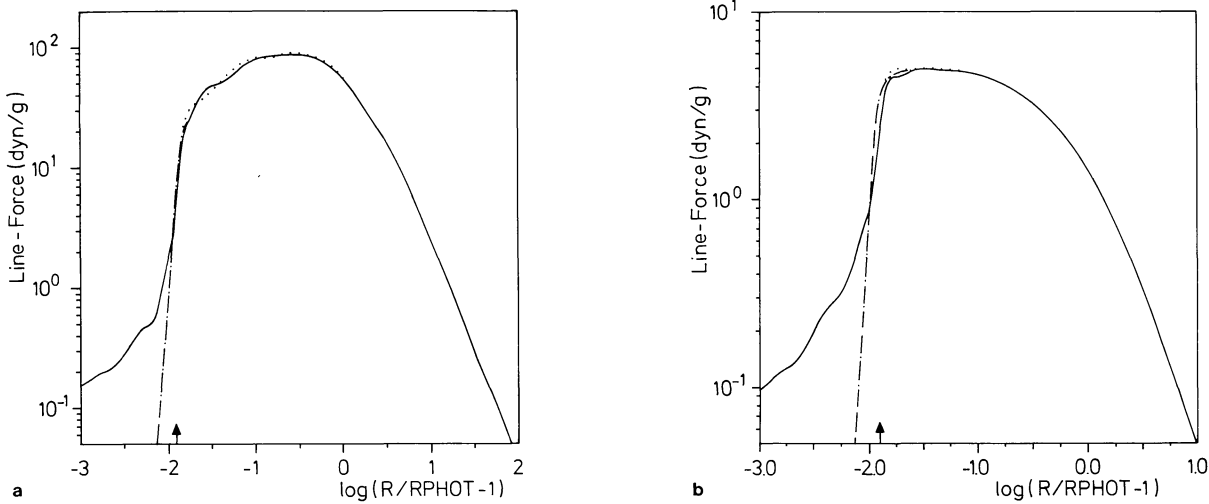


**Fig. 5a and b.** Line acceleration for a strong (a) and a weak (b) line. The fully drawn curve is evaluated with the CMF method, dashed-dotted is the SA with correct continuum intensity and dotted is the SA with core-halo structure and no limb-darkening (The arrow indicates the sonic point)

SA-forces always go to zero for  $\tau_s \rightarrow \infty$ , which corresponds to  $r \rightarrow R_*$ .

This difference is however not crucial, since in these regions the radiation force due to continuum processes (true absorption and Thomson scattering) will dominate the line force by a large factor. We have verified that in the deepest layers the continuum force is 90–95% of the total force.

Therefore the most important difference lies in that part of the atmosphere where the mass loss is determined, the neighbourhood of the sonic point. Below this point the CMF force is smaller, while above it is larger than the corresponding SA forces. The main effect of this difference is to lead to a steeper velocity gradient, as discussed in Sect. 4.4.

Another point which is clearly demonstrated in Fig. 5 is that, as long as the photospheres are not extended, the assumption of a core-halo structure and no limb-darkening is a good one, because the two SA forces are essentially the same, although one is evaluated with the exact continuum intensity whereas the other makes use only of the emergent flux at large radii.

#### 4.2. Representation of the total line force by a statistical sample

As we are not able to solve the line transfer equations for each of the 200000 lines of Abbott's list at present, we have used a simple statistical method to represent the total line force by only a few lines and renormalized the force obtained in this way by a factor which leads to agreement of the MCAK-force and the CMF force in the outer regions, where the SA is fully justified (compare the previous section).

As first realized by CAK (1975), their force multiplier

$$M(t) = \sum_{\text{lines}} \frac{F_c(v) \Delta v_D}{F} \min(\eta_L, 1/t),$$

with line strengths

$$\eta_L = \frac{\bar{\kappa}_L}{\sigma_{TH}} \quad (\eta_L = 1/\beta \text{ in the notation of CAK})$$

can be represented by a line distribution function

$$dN = -N_0 \eta_L^{\alpha-2} d\eta_L \frac{dv}{v}, \quad (43)$$

if

$$N_0 = kc(1-\alpha)/v_{th}, \quad (44)$$

with the CAK parameters  $k$  and  $\alpha$  and the thermal Doppler velocity  $v_{th}$ . Therefore, one gets for the number of lines in the wavelength interval  $(\lambda_{\max}, \lambda)$  and line-strength interval  $(\infty, \eta_L)$

$$N(\lambda, \eta_L) = \frac{c}{v_{th}} k \alpha \eta_L^{\alpha-1} \ln \left( \frac{\lambda_{\max}}{\lambda} \right). \quad (45)$$

For our line statistics, we choose  $\lambda_{\max} = 10000 \text{ \AA}$ , 3 different line strengths  $\eta_L = 10^6, 10^4, 10^2$  (strong, intermediate and weak lines), three frequency points at the maximum ( $v_{\max}$ ) of the Planck-function, longward ( $v_-$ ) and shortward ( $v_+$ ) of this, so that  $B_{v_{\pm}} = 0.5 B_{v_{\max}}(T_{\text{eff}})$ .

In order to represent Abbott's force multiplier, after calculating for each of these 9 lines the CMF force and multiplying this by the appropriate number of lines, the whole force has to be multiplied by the radius dependent factor  $(n_E/W)^\delta$  to account for ionization and dilution. This force has by construction to be the same as the MCAK force in the outer parts, up to a factor of order unity which originates in the slightly different emergent fluxes (Abbott used Kurucz fluxes, whereas we have a simple hydrogen atmosphere) and the rather extreme attempt to represent 200000 lines by an ensemble of 9 lines. To obtain this renormalization constant, we compare for a given velocity field both the MCAK force and the total CMF line force from the statistical procedure at large radii and fix the result then for all times. It turned out that the value of this factor is 0.9 to 1.1 for hot stars ( $40000^\circ - 50000^\circ$ ) and of order 0.7 for cooler ones ( $20000^\circ - 30000^\circ$ ). In this way we can insure that we deal with radiative acceleration laws that are essentially identical well outside the sonic point, so that we can study the effect of the SA in the inner parts of the atmosphere.

### 4.3. Construction of a selfconsistent stellar wind model using the CMF force

After having described the calculation of the total CMF line force and its renormalization to the MCAK force in the outer parts of the atmosphere, we will now discuss the construction of a self-consistent stellar wind model using this force.

As initial values for  $v(r)$  and  $\rho(r)$  we use an appropriate MCAK model with photospheric radius at  $\tau_{Th} = 10$  and calculate the radiation transport. For the continuum, we assume a pure (fully ionized) hydrogen atmosphere (in LTE) and find a temperature structure from Eq. (1) with  $\bar{x}_H$  as flux weighted bound-free, free-free and Thomson-scattering opacities. Note that the  $bf$  and  $ff$  continuum opacity is taken into account only for the temperature distribution and the line radiative transfer (to assess proper thermalization), but not for the radiative force. In this way we keep the same continuous force as in the MCAK theory and investigate the SA only. In future work true absorption will be included in the radiative force. Line transitions are approximated by a two-level atom with constant line strength, so that  $\bar{x}_L = \eta_L \sigma_{TH}(r)$ . Assuming complete redistribution and only Doppler broadening we obtain for the line source function  $S_L$

$$S_L(r) = (1 - \varepsilon(v, r)) \int J_\nu(r) \Phi(v, r) dv + \varepsilon(v, r) B_\nu(r) \quad (46)$$

with  $\varepsilon(v, r)$  the LTE parameter in the hydrogenic approximation. As explained above, we use as the lower boundary condition the diffusion approximation at  $\tau_{Th} = 10$ , which corresponds to an optical depth in the continuum from 20 . . . 100, depending on the wavelength.

From the solution of the continuum and line transfer equations we obtain the total radiative acceleration, which is now put into a hydrodynamic code to obtain a new velocity and density structure. This code solves Eq. (3) from the sonic point up- and downwards and fixes the mass loss rate from the condition

$$\tau_{TH} = \int_{R_*}^{\infty} \sigma_{TH} dr = 10. \quad (47)$$

The advantage of this procedure is that we use as the boundary condition the only physically relevant point – the sonic point – and not the somewhat artificial critical point of the MCAK theory. Our integrations are continued up to  $R_{max} = 100 R_*$ , for we found that the change in velocity gradient is negligible only beyond  $6-10 R_*$ .

With the new velocities and densities we solve again the transfer equations, and the process is iterated. A somewhat disturbing detail is the sensitivity of the mass loss rate to the location of the sonic point. Since this point is situated much closer to the photosphere than the critical point and the whole solution depends on its location, a small change in the radiation force can lead to a drastic change in the velocity – and therefore density structure. Nevertheless we can obtain convergence by inserting

a Newton-Raphson extrapolation at *each* radius point after 3–4 iteration cycles in order to avoid too large oscillations in the convergence process. With this trick we obtained, with 20–25 iteration cycles on the average, convergence in velocity of 1–3% at *each* radius point.

### 4.4. Results for the 05f-“CAK”-star

In this section we will compare the final stellar wind model for the CAK-star calculated with the CMF method to that calculated with the MCAK theory. The parameters  $k$ ,  $\alpha$  and  $\delta$  which are used in both theories are given in Sect. 3.3 (see also 5), the corresponding number of lines obtained by our statistics are presented in Table 3. We obtained the following results:

	MCAK	CMF	
$\dot{M}$	6.67	6.40	$(10^{-6} M_\odot/\text{yr})$
$v_\infty$	2915	2854	$(\text{km s}^{-1})$

From Fig. 6 we see that not only the global wind parameters, but the whole wind structure are in good agreement.

The only deviation is a slightly steeper velocity gradient in the CMF model which arises because the total line force has a different behaviour near the sonic point (see Sect. 4.1).

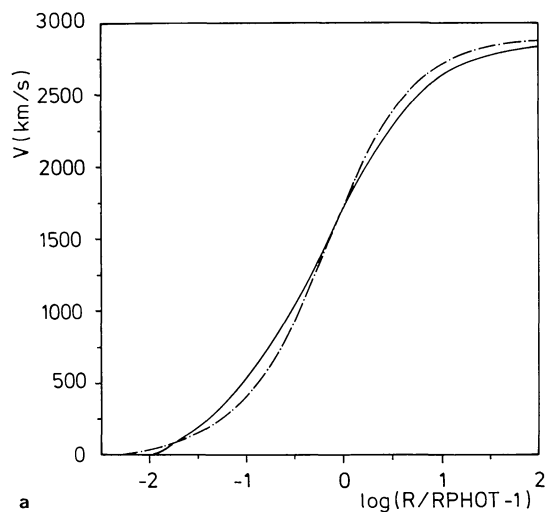
On the other hand, Weber (1981) found in his CMF-solutions a flatter velocity field compared with the ordinary CAK-theory. This is not surprising, since as described in Sects. 3.2 and 3.3 the CAK theory in the pure radial streaming approximation without CF yields an essential steeper velocity field than the correct treatment.

Comparing our results with those by Weber, another point has to be mentioned. When we started our work with the CMF formalism, we recalculated Weber’s model with the same parameters he used. To our surprise we obtained a different solution than he; in particular our mass loss rates were nearly a decade smaller than the values he quoted. Working with such complex codes, it is of course hard to decide on which side the error is. However, as our CMF results are close to those obtained with the MCAK theory, which has quite another solution formalism, we feel that we can trust them.

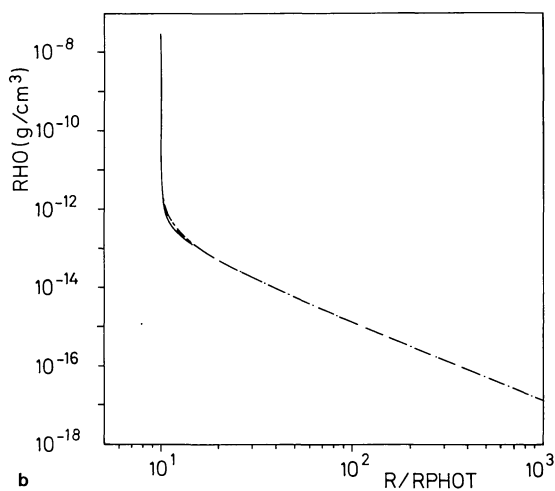
Although our results at the moment seem to prove that the approximations of the MCAK theory – Sobolev approximation, core-halo-structure, no limb-darkening – are of little importance, we think that it is necessary to continue the much more sophisticated CMF theory for the following reasons. First, we cannot be completely sure that the agreement is simply caused by the renormalization procedure itself, which fixes the CMF calculations in the outer layers. Second, we feel that in the case of extended photospheres as for WR-stars (see Pauldrach et al., 1985) and extreme supergiants the CMF calculations will be clearly more appropriate. Therefore, the calculation of selfconsistent

**Table 3.** Statistically derived number of lines for the “CAK-star”

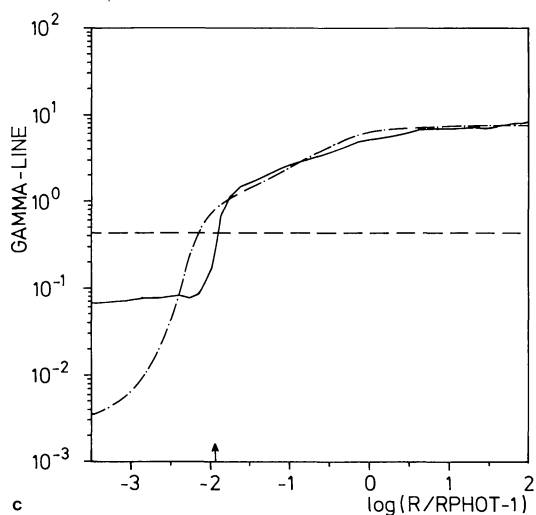
	539 < $\lambda$ < 1034	1034 < $\lambda$ < 3463	3463 < $\lambda$ < 10000
$\infty > \eta_L > 10^6$	13	24	16
$10^6 > \eta_L > 10^4$	55	103	68
$10^4 > \eta_L > 10^2$	290	539	358



a



b



c

**Fig. 6a–c.** Comparison of the MCAK (dashed-dotted) and CMF (fully drawn) calculations for the O5f-star. **a** shows the velocity field, **b** the density structure and **c** the ratio of line- to gravitational acceleration. The sonic point is indicated by the arrow

wind models using CMF and Abbott's full line list will be part of our future work. This will also allow us to investigate in a realistic way the effects of multiple scattering on the velocity field.

#### 4.5 The photospheric line force

In the non-LTE model photospheres which are normally used for a detailed spectroscopic determination of the stellar parameters such as effective temperature, gravity and helium abundance (for a recent review see Kudritzki and Hummer (1985) or Kudritzki (1985)) the influence of the photospheric line force on the density stratification is neglected. In these hydrostatic models only the contributions to the effective gravity of Thomson scattering, free-free and bound-free absorption are taken into account. The usual argument is that the strategic lines like  $H\gamma$ ,  $\text{He I } \lambda 4471$ ,  $\text{He II } \lambda 4542$  are formed in the subsonic photospheric region (see Kudritzki, 1980; Kudritzki et al., 1983), where the effects of the

velocity field on the density structure are negligible. However, this argument does not hold as far as the line force is concerned, for the following reasons:

Since the opacity of a metal line increases drastically as soon as the outflow velocity  $v(r)$  becomes larger than the thermal velocity  $v_{th}^{metal}$  of the ion, and since the sound velocity  $v_s$  of the photospheric plasma is larger than  $v_{th}^{metal}$  by at least a factor of three for the relevant ions, we have a subsonic ("quasi-hydrostatic") photospheric region, where

$$v_{th}^{metal} \leq v(r) \leq v_s. \quad (48)$$

and where the velocity field becomes important indirectly due to its influence on radiative force and the effective gravity. Moreover, even in regions where  $v(r) \leq v_{th}^{metal}$  the line force might be important if the radiation field is not yet thermalized.

We have examined this effect for the case of the low gravity object  $\zeta$  Puppis, which has been recently studied spectroscopically by Kudritzki et al. (1983) and Bohannan et al. (1985), and calculated a CMF stellar wind model with  $T_{eff} = 42000$  K,  $\log g = 3.65$  and  $R = 19.5 R_{\odot}$ , which with  $\dot{M} = 7.0 \cdot 10^{-6} M_{\odot}/\text{yr}$  and  $v_{\infty} = 2100 \text{ km s}^{-1}$  yielded wind parameters close to the observed ones.

Figure 7 demonstrates how the effective gravity is influenced by the line force, which is calculated in the CMF for a statistical sample of lines as described in the foregoing sections. In the subsonic region from the sonic point down to  $n_e = 10^{15} \text{ cm}^{-3}$ , where the far UV radiation field starts thermalizing, the line force significantly reduces the effective gravity. In view of modern observational techniques, which allow the measurement of extremely accurate line profiles and by this a precise determination of stellar parameters from "photospheric lines" (see Bohannan et al., 1985), it appears to be worthwhile to investigate this effect in more detail (using improved non-LTE continuum opacities and a realistic line list) to avoid systematic errors in the gravity determination.

#### 5. A first comparison with observations

Despite our approximations, the results we obtained in Sect. 3.3 and 4.5 were most encouraging and led us to apply the theory to a representative sample of galactic OB-stars, comparing the

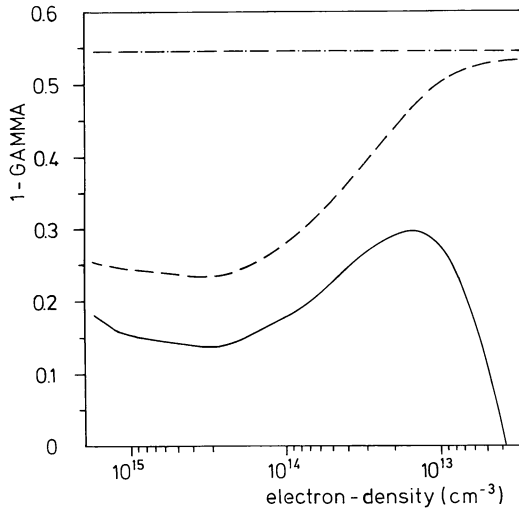


**Fig. 7.** Effective gravity (in units of the gravity  $g$ ) as function of local electron density in the atmosphere for a model with  $T_{\text{eff}} = 42000$  K,  $\log g = 3.65$  and  $R = 19.5 R_{\odot}$ . Dashed-dotted: Radiative acceleration by Thomson scattering only; dashed: Thomson scattering plus bound-free and free-free absorption; fully drawn: Thomson scattering, bound-free, free-free and line absorption. The sonic point is at  $n_e \approx 3.5 \cdot 10^{12} \text{ cm}^{-3}$ , where the fully drawn curve crosses the zero line

calculated values of  $\dot{M}$  and  $v_{\infty}$  with the observations. For our calculations we have chosen 3 OV-stars, 2 evolved O-stars and 2 B-supergiants, all with well known wind parameters and not too uncertain values of  $T_{\text{eff}}$ ,  $\log g$  and  $R_{*}$ . Since from our investigations we know that the wind parameters  $\dot{M}$  and  $v_{\infty}$  show a significant dependence on the stellar parameters  $T_{\text{eff}}$ ,  $\log g$  and  $R_{*}$ , we have adjusted the latter within the allowed limits of errors. This procedure allows us to investigate whether the observed stellar wind parameters can be explained in principle by the improved theory or not. An improved determination of the stellar parameters in the future, which is at hand with present day observational techniques, will of course lead to more precise constraints on the theory.

Before discussing our results we have to explain how the radiative line force was calculated for the individual objects. For this purpose, we used Table 2 of the paper by Abbott (1982) and derived the necessary constants  $k$ ,  $\alpha$ ,  $\delta$  by the following iterative

procedure: With a first guess of  $\alpha$ ,  $\delta$ ,  $k$  we determined the relevant domain in the  $(t, n_E/W)$ -plane (see Eq. 26) for the individual star. Then final values of  $\alpha$ ,  $\delta$ ,  $k$  were fitted to reproduce the tabulated force multiplier values just in this relevant domain. These values are given in Table 4. We found, however, that the steps tabulated in  $n_E/W$  by Abbott are too large to allow very accurate interpolation ( $\Delta \log n_E/W = 3$ ). While this was not a problem in wind regions above the sonic point ( $t = 10^{-4}$  to  $10^{-2}$ ) where we were always close to  $\log n_E/W \approx 1$ , which is tabulated, we feel somewhat uncertain for deeper layers ( $t = 10^{-1}$ ), where  $n_E/W$  was often just between the values of the last tabulated steps. Moreover, it is not completely clear, whether the representation of  $M(t)$  by one set of  $\alpha$ ,  $k$ ,  $\delta$  is really sufficient, in particular in deeper layers. This will be investigated in the future by more refined force multiplier calculations.

Table 5 gives the result of the calculations obtained from both our MCAK and CMF theory together with the observed values  $\dot{M}_{\text{obs}}$  and  $v_{\infty}^{\text{obs}}$  and the adopted stellar parameters. In addition, the values  $\dot{M}_{\text{SR}}$  and  $v_{\infty}^{\text{SR}}$  using the scaling relations of section IV.4 are quoted together with the velocity field parameter  $\beta$  according to Eqs. 33 and 35. Strikingly, the agreement between theory and observations is very good for all of the objects in Table 5. We can reproduce roughly the observed mass-loss rates and terminal velocities not only for the O main-sequence stars and the evolved O-stars but also for such an extreme object like P-Cygni, which has a very high  $\dot{M}$  and an extremely low  $v_{\infty}$ . These results encourage us to improve the theory further and to carry out more refined comparisons with observation (see the following section).

**Table 4.** Values of  $k$ ,  $\alpha$ , and  $\delta$  used in the MCAK theory

$T_{\text{eff}}$	$k$	$\alpha$	$\delta$
20000	0.32	0.565	0.02
30000	0.17	0.59	0.09
40000	0.124	0.64	0.07
50000	0.124	0.64	0.07

**Table 5**

Star	Spectral type	$T_{\text{eff}}$ ( $10^3$ K)	$\log g$	$R/R_{\odot}$	$\dot{M}_{\text{obs}}$ ( $10^{-6} M_{\odot}/\text{yr}$ )	$\dot{M}_{\text{MCAK}}$ ( $10^{-6} M_{\odot}/\text{yr}$ )	$\dot{M}_{\text{CMF}}$ ( $10^{-6} M_{\odot}/\text{yr}$ )	$\dot{M}_{\text{SR}}$ ( $10^{-6} M_{\odot}/\text{yr}$ )	$v_{\infty}^{\text{obs}}$ km s $^{-1}$	$v_{\infty}^{\text{MCAK}}$ km s $^{-1}$	$v_{\infty}^{\text{CMF}}$ km s $^{-1}$	$v_{\infty}^{\text{SR}}$ km s $^{-1}$	$\beta$	Notes
P-Cyg	BIIa	18.0	2.0	68.	20–30	29	24.2	21.6	400	395	395	426	0.98	1
$\epsilon$ -Ori	B0Ia	28.5	3.25	37.	3.1	3.3	3.4	3.19	2010	1950	1930	1905	0.72	2
$\zeta$ -OriA	O9.5I	30.0	3.45	29.	2.3	1.9	1.7	1.86	2290	2274	2140	2250	0.72	2
9-Sgr	O4(f)V	50.0	4.08	12.	4.0	4.0	3.4	4.12	3440.	3480	3540	3440	0.81	3
HD 48099	O6.5V	39.0	4.00	11.	0.63	0.64	0.7	0.67	3500.	3540	3150	3230	0.81	4
HD 42088	O6.5V	40.0	4.05	5.8	0.13	0.20	0.23	0.203	2600.	2600.	2320	2540	0.79	4
$\lambda$ -Cep	O6ef	42.0	3.7	17.	4.0	5.1	4.0	4.98	2500.	2500.	2470	2400	0.79	4

Notes: 1 Lamers, H.J.G.L.M. et al. (1983), 2 Abbott, D.C. et al. (1980), Abbott (1978), 3 Abbott, D.C. et al. (1984), 4 Garmany, C. et al. (1981)

## 6. Conclusions and future work

The reasonable agreement between the improved selfconsistent theory and the observations, in both  $\dot{M}$  and  $v_\infty$  which we obtained over a rather large domain in the HR-diagram, indicates that the concept of radiation driven winds is surely very promising for a quantitative description of the time-averaged stationary wind properties of hot luminous stars. However, a variety of additional steps will have to be undertaken in the future before the theory can be regarded as really reliable in a quantitative sense: We will have to test whether the wind properties of O-stars in the Magellanic Clouds, which are different from those of their galactic counterparts (see Conti and Garmany, 1985), can also be reproduced by the theory. For this purpose new force multipliers for O-stars with significantly lower metal content are presently being calculated in our group. This will allow us to apply the theory on the LMC and SMC O-stars. In the calculation of force multipliers the treatment of ionization and excitation will have to be improved by following the direction out lined by Abbott and Lucy (1985), as well as by checking the influence of low lying autoionization levels (Nußbaumer and Storey, 1983, 1984, 1985). Moreover, the concept of representing the force multiplier throughout the total atmosphere by one single set of  $k$ ,  $\alpha$ ,  $\delta$  will have to be reexamined carefully.

The CMF calculations will have to be extended using a realistic non-LTE continuum opacity and temperature stratification plus a realistic line list so that no renormalization procedures are needed. Such calculations appear to be feasible now and will represent something like a final stage of the theory (within the limits of stationarity and radiative equilibrium). They will allow us to investigate the influence of multiple scattering on both  $\dot{M}$  and  $v_\infty$  in a realistic way. In addition, these computations will be very useful to understand in detail the extended atmospheres of WR-stars (see Pauldrach et al., 1985) and extreme supergiants of spectral type O, B, A. They will allow us to overcome the artificial separation between photosphere and stellar wind region and will provide us with unified hydrodynamic model atmospheres, which then can be tested by detailed spectroscopy of these astronomically extremely important objects.

*Acknowledgements.* We gratefully acknowledge the help of Dr. W.R. Hamann (Kiel) during the development of our CMF-code. We also thank Dr. D.G. Hummer for his encouraging continuous interest, fruitful stimulating discussions and careful reading of the manuscript. The critical remarks by Dr. D.C. Abbott are also gratefully acknowledged.

## Appendix

Here we present the principles of solving the MCAK equation of motion (27). As our method is in some regards similar to the procedure of CAK, the reader should have in mind their derivations.

Since Eq. (27) is considerably complicated because of the correction factor  $K(r, w, w')$ , an iteration scheme is required. For the first iteration only the  $r$ -dependence of  $K$  was kept. This yields

$$K(u) = \begin{cases} (1 - (1 - R_*^2 u^2)^{\alpha+1}) / ((\alpha + 1) R_*^2 u^2) & \text{for } r > R_* \\ 1 / (\alpha + 1) & \text{for } r \leq R_* \end{cases} \quad (\text{A1})$$

In the next iteration steps the updated  $w'(u)$  and  $w(u)$  are inserted in the correct  $K$  (Eq. (25)), and the equation of motion (in the form

described below) is solved again. As is seen in Fig. 3, which shows the CAK approximation  $K \equiv 1$  and three subsequent iteration steps, convergence is achieved rapidly. It should be noted that, as Eq. (A1) already gives  $\dot{M}$  and consequently  $\rho(r)$  very well, an internal iteration cycle for the temperature structure (Eq. 1) can be started after the first  $K(u)$  step.

For the solution of the MCAK Eq. (27), which is a nonlinear equation in  $w'$ , an integrable form is useful, which can be obtained from the total derivative of (27) with respect to  $w' = z$ . Therefore,

$$\begin{aligned} du/dz &= -F_z / (F_u + F_w z), \\ dw/dz &= -z F_z / (F_u + F_w z) = z du/dz, \\ F_u + F_w z &\neq 0, \\ F_u &= -(z/2w) da^2/du - dh/du - Cz^\alpha \partial f / \partial u, \\ F_w &= za^2/2w^2 - Cz^\alpha \partial f / \partial w, \\ F_z &= (1 - a^2/2w) - \alpha C f z^{\alpha-1}, \\ f(u, w) &= G(u) w^{-\delta/2}. \end{aligned} \quad (\text{A2})$$

$G(u)$  is calculated according to the expression for  $G$  in Eq. (27) using the values of  $w, w'$  from the foregoing iteration. Thus, with respect to the derivatives in Eqs. (A2), (A3), (A4) only the  $u$ -dependence is formally taken into account.

It can easily be verified that the singularity in (A2) (vanishing numerator and denominator) yields exactly in the singular condition (numerator)

$$\partial F(u, w, w') / \partial w' = 0 \quad (\text{A3})$$

and in the regularity condition (denominator)

$$(\partial F / \partial u)_c + w'_c (\partial F / \partial w)_c = 0 \quad (\text{A4})$$

as defined by CAK.

Inserting (27) in (A4) and making use of (A3) and the separable form of  $f(u, w)$ , one gets after some calculation

$$\begin{aligned} w_c &= a^2/2 - (\alpha/(1-\alpha))h/(B/2a^2 + ((B/2a^2)^2 + 2C_1/a^2)^{1/2}), \\ z_c &= B/4 + ((B/4)^2 + a^2 C_1/2)^{1/2} - h\alpha/(1-\alpha), \\ C &= -(1/(1-\alpha))hw_c^{\delta/2}/(G(u)z_c^2), \\ B &= da^2/du + \delta h/(1-\alpha), \\ C_1 &= dh/du - h(dG/du)/(G(u)(1-\alpha)), \end{aligned} \quad (\text{A5})$$

and thus the critical values  $w_c$  and  $w'_c$  as well as the eigenvalue of the system  $\dot{M}$  (see Eq. 27).

Finally (A2) is given at the critical point by

$$\begin{aligned} (du/dz)_c &= E/2D + (E^2 + 4DF)^{1/2}/2D \\ (dw/dz)_c &= (z_c du/dz)_c \end{aligned} \quad (\text{A6})$$

with

$$\begin{aligned} D &= (a^2 z^3 / w^3 - (z^2 / w^2)(da^2/du + h\delta(\delta/2 + 1)/(2(1-\alpha))) \\ &\quad + (z/w)((d^2 a^2/du^2)/2 + \delta h(dG/du)/(G(u)(1-\alpha))) \\ &\quad + d^2 h/du^2 - h(d^2 G/du^2)/(G(u)(1-\alpha))), \\ E &= (3a^2 z/2w^2 - (da^2/du)/w + 2\alpha h(dG/du)/(zG(u)(1-\alpha)) \\ &\quad - (2\alpha + 1)\delta h/(2w(1-\alpha))), \\ F &= (-\alpha h/z^2)_c \end{aligned}$$

In order to integrate Eq. (A2) in each direction from the singular point, only the critical radius  $u_c$  remains to be calculated.

This is done by using the additional boundary condition ( $u_p$  is the photospheric point defined by a specified optical depth, see Sect. 2):

$$1 - (\dot{M}\sigma_e/(4\pi 2^{1/2})) \int_{u_p}^0 w^{-1/2} du = 0 \quad (\text{A7})$$

and an iterative procedure, which starts with an initial guess.

This guess can be obtained in the following way: With

$$-a^2/u_c \ll GM(1 - \Gamma) =: A, \quad (\text{A8})$$

which is surely true up to the singular radius, we find from (A5) for  $z_c$

$$z_c = -\frac{\delta A}{4b} + \left( \left( \frac{\delta A}{4b} \right)^2 + \frac{a^4}{u^2} + \frac{AG'a^2}{2bG} \right)^{1/2} + \frac{A\alpha}{b} \quad (\text{A9})$$

where  $b = 1 - \alpha$ . Comparing the orders of magnitude of the terms in (A9) we find

$$z_c \approx A\alpha/b. \quad (\text{A10})$$

From Eq. (27) we find that between the sonic point  $u_s$  and the critical point  $u_c$  we have  $z \approx z_c = \text{const.}$  (see also CAK, Abbott (1978) or Eq. (A17)). By integration we therefore obtain

$$w_c = \frac{A\alpha}{b} (u_c - u_p), \quad (\text{A11})$$

where we have used the fact that  $u_p \approx u_s$ . Setting (A11) equal to (A5) (for which (A8) and  $a^2 \ll w^2$  is taken into account) we obtain a cubic equation for the critical point  $u_c$ :

$$\begin{aligned} u_c^3(\bar{C} - 2\bar{B}) + u_c^2(3 - 2\bar{C}\bar{D} + 2\bar{B}\bar{D} + 2u_p(\bar{B} - \bar{C})) \\ + u_c(\bar{C}u_p^2 - 8\bar{D} + \bar{C}(\bar{D}^2 + 2u_p\bar{D}) - 8u_p) + 4u_p^2 \\ + 4\bar{D}^2 + 8u_p\bar{D} = 0 \end{aligned} \quad (\text{A12})$$

$$\bar{B} = \frac{\delta A}{2a^2b}, \quad \bar{C} = \frac{2AG'u_c}{a^2bG}, \quad \bar{D} = \frac{a^2b}{2A\alpha}$$

Eq. (A11) is solved by transformation to the Cardan's form. (Note that the  $u$ -dependence of  $\bar{C}$  is dropped by setting  $-u_c = 1/(1.05 R_*)$ ).

In the scaling relation for  $v_\infty$  (Eq. 35) a simple estimate is needed for the critical velocity  $v_{\text{crit}}$  (Eq. 32). This is obtained from the equation of motion (Eq. 27) assuming the critical point to lie not too far from  $R_*$  so that  $K(u, w, w')$  is represented in first order by (Eq. A1). Assuming in addition again  $a \ll v(r)$ ,  $v_{\text{esc}}$  one obtains a simplified equation of motion, which is approximately valid between for  $R_* < r < 2R_*$ :

$$\begin{aligned} w' = -A + C^*(w)^\alpha w^{-\delta/2} \cdot K(u) \\ C^* = C(R_*^2)^{-\delta} \end{aligned} \quad (\text{A13})$$

From the singularity and regularity condition (A2) we then obtain again Eq. (A10) and

$$\frac{z_c}{w_c} = \frac{2R_* (1 - u_c^2 R_*^\alpha (1 + \alpha u_c^2 R_*^\alpha)) - 1}{\delta/2 \cdot u_c R_* (1 - (1 - u_c^2 R_*^\alpha)^{\alpha+1})} \quad (\text{A14})$$

Expanding (A10) in  $(1 - u_c^2 R_*^\alpha)$  and neglecting terms of order unity, one gets

$$\begin{aligned} \frac{w'}{w} \approx \frac{2R_*}{\delta/2} f_c(u_c) \\ f_c(u_c) = 1 - (1 + \alpha)(1 - u_c^2 R_*^\alpha)^\alpha, \end{aligned}$$

which leads with the approximate critical radius of  $u_c = -1/1.04 R_*$  directly to the estimate for  $v_{\text{crit}}$  in Eq. (32).

## References

- Abbott, D.C.: 1978, *Astrophys. J.* **225**, 893  
 Abbott, D.C.: 1980, *Astrophys. J.* **242**, 1183  
 Abbott, D.C., Bieging, J.H., Churchwell, E., Cassinelli, J.P.: 1980, *Astrophys. J.* **238**, 196  
 Abbott, D.C.: 1982, *Astrophys. J.* **259**, 282  
 Abbott, D.C.: 1986, 3rd Trieste Workshop, Sac Peak, August 1984, invited paper (in press)  
 Abbott, D.C., Bieging, J.H., Churchwell, E.: 1982, *IAU Symp. No. 99*, 215  
 Abbott, D.C., Teleso, C.M., Wolff, S.C.: 1984a, *Astrophys. J.* **279**, 225  
 Abbott, D.C., Bieging, J.H., Churchwell, E.: 1984, *Astrophys. J.* **280**, 671  
 Abbott, D.C.: 1979, *IAU Symp. 83*, p. 237, ed. P.S. Conti and C.W.H. de Loore  
 Abbott, D.C., Hummer, D.G.: 1985, *Astrophys. J.* **294**, 286  
 Abbott, D.C., Lucy, L.B.: 1985, *Astrophys. J.* **288**, 679  
 Bohannan, B., Abbott, D.C., Hummer, D.G., Voels, S.A.: 1985, in *Luminous Stars and Associations in Galaxies*, Proc. of IAU Symp. 116, eds. C. de Loore, A. Willis, P. Laskarides  
 Castor, J.: 1974, *Monthly Notices Roy. Astron. Soc.* **169**, 279  
 Castor, J., Abbott, D., Klein, R.: 1975, *Astrophys. J.* **195**, 157  
 Castor, J., Lamers, H.J.G.L.M.: 1979, *Astrophys. J. Suppl.* **39**, 481  
 Castor, J.: Symposium No. 83, 175  
 Conti, Garmany: 1985, *Astrophys. J.* **293**, 407  
 Friend, D., Castor, J.: 1983, *Astrophys. J.* **272**, 259  
 Friend, D., Mac Gregor: 1984, *Astrophys. J.* **282**, 591  
 Garmany, C.: 1981, *Astrophys. J.* **250**, 660  
 Garmany, C., Conti, P.: 1984, *Astrophys. J.* **284**, 705  
 Henrichs, H.: 1984, Proc. 4th Europ. IUE Conf., ESA Sp-215, p. 43  
 Howarth and Prinja, 1985, *Monthly Notices Roy. Astron. Soc.* (in press)  
 Hummer, D.G., Rybicki: 1985, *Astrophys. J.* **293**, 258  
 Hummer, D.G., Puls, J.: in prep.  
 Klein, R., Castor, J.: 1978, *Astrophys. J.* **220**, 902  
 Kudritzki, R.P.: 1980, *Astron. Astrophys.* **85**, 174  
 Kudritzki, R.P., Hummer, D.G.: 1985, Intrinsic Properties of Hot Blue Stars, Proc. of IAU Symp. 116 on "Luminous Stars and Associations in Galaxies", eds. C. de Loore, A. Willis, P. Laskarides  
 Kudritzki, R.P., Simon, K.P., Hamann, W.R.: 1983, *Astron. Astrophys.* **118**, 245  
 Kudritzki, R.P.: 1985, Quantitative Spectroscopy of Very Hot Stars, Proc. of ESO Workshop on "Production and Distribution of C, N, O Elements", eds. Danziger et al.  
 Lamers, H.J.G.L.M., Morton, D.: 1976, *Astrophys. J. Suppl.* **32**, 715  
 Lamers, H.J.G.L.M.: 1984, *Astron. Astrophys.* **134**, L17  
 Lamers, H.J.G.L.M.: 1983, *Astron. Astrophys.* **128**, 299  
 Landstreet, J.D.: 1982, *Astrophys. J.* **85**, 611  
 Leroy, M., Lafon, J.-P.J.: 1982, *Astron. Astrophys.* **106**, 345  
 Lucy, L.B., Solomon, P.: 1970, *Astrophys. J.* **159**, 879  
 Lucy, L.B.: 1971, *Astrophys. J.* **163**, 95  
 Lucy, L.B., White, R.: 1980, *Astrophys. J.* **241**, 300  
 Lucy, L.B.: 1982a, *Astrophys. J.* **255**, 278

- Lucy, L.B.: 1982b, *Astrophys. J.* **255**, 286  
Lucy, L.B.: 1983, *Astrophys. J.* **274**, 372  
Lucy, L.B.: 1984, *Astron. Astrophys.* **140**, 210  
Mihalas, D., Kunasz, P., Hummer, D.G.: 1975, *Astrophys. J.* **202**, 465  
Mihalas, D., Kunasz, P., Hummer, D.G.: 1976, *Astrophys. J.* **206**, 515  
Nußbaumer, H., Storey, P.J.: 1983, *Astron. Astrophys.* **126**, 75  
Nußbaumer, H., Storey, P.J.: 1984, *Astron. Astrophys. Suppl.* **56**, 293  
Nußbaumer, H., Storey, P.J.: 1985, *Astron. Astrophys. Suppl.* (submitted)  
Panagia, N., Macchetto, F.: 1982, *Astron. Astrophys.* **106**, 266  
Pauldrach, A., Puls, J., Hummer, D.G., Kudritzki, R.P.: 1985, *Astron. Astrophys.* **148**, L1  
Weber, S.: 1981, *Astrophys. J.* **243**, 954